1-1-2009

On Coverage and Capacity for Disaster Area Wireless Networks Using Mobile Relays

Wenxuan Guo

Xinming Huang
Worcester Polytechnic Institute, xhuang@wpi.edu

Hindawi Publishing Corporation
EURASIP Journal on Wireless Communications and Networking
Volume 2009, Article ID 251314, 17 pages
doi:10.1155/2009/251314

Research Article

On Coverage and Capacity for Disaster Area Wireless Networks Using Mobile Relays

Wenxuan Guo and Xinming Huang

Department of Electrical and Computer Engineering, Worcester Polytechnic Institute, 100 Institute Road, Worcester, MA 01609, USA

Correspondence should be addressed to Wenxuan Guo, wxguo@wpi.edu

Received 11 June 2009; Accepted 8 September 2009

Recommended by George Karagiannidis

Public safety organizations increasingly rely on wireless technology to provide effective communications during emergency and disaster response operations. This paper presents a comprehensive study on dynamic placement of relay nodes (RNs) in a disaster area wireless network. It is based on our prior work of mobility model that characterizes the spatial movement of the first responders as mobile nodes (MNs) during their operations. We first investigate the COverage-oriented Relay Placement (CORP) problem that is to maximize the total number of MNs connected with the relays. Considering the network throughput, we then study the CApacity-oriented Relay Placement (CARP) problem that is to maximize the aggregated data rate of all MNs. For both coverage and capacity studies, we provide each the optimal and the greedy algorithms with computational complexity analysis. Furthermore, simulation results are presented to compare the performance between the greedy and the optimal solutions for the CORP and CARP problems, respectively. It is shown that the greedy algorithms can achieve near optimal performance but at significantly lower computational complexity.

1. Introduction

Public safety organizations increasingly rely on wireless technology to establish disaster area communication systems for first responder operations. The reason mainly lies in the fact that in catastrophe situations, wired network suffers from low sustainability, high expense, slow deployment, and being unadaptable to mobility. It is crucial for the replacement network to be highly dynamic in accordance with the mission-critical mobile users. Considering the first responders as mobile nodes (MNs), the communication range of each MN is often limited by its power constraint. Since MNs are highly mobile within the disaster area, using infrastructureless ad hoc networks would result in unexpected disconnection for some MNs and frequent rediscovery of routing paths. Therefore, mobile relay nodes (RNs) can be introduced to relay the communications between MNs and the base station. In this paper, we exemplify the movable RNs as vehicles loaded with wireless communication equipment. The RNs installed on wheeled vehicles move themselves to places where the first responders are actively working in the field. Although RNs form the backbone network, the number of users each RN can support is often limited, because each RN can only provide limited number of channels. Due to the abundance of available bandwidth in disaster area, we assume that each RN can set its bands at unused frequencies, so that they do not interfere with each other. With MNs and RNs defined, we term such a dynamic communication system as a disaster area wireless network (DAWN), shown in Figure 1.

In our prior work [1], we proposed a mobility model to describe the movement pattern of MNs within a large disaster area. Moreover, we studied the coverage problem with no capacity constraints on RNs. In this paper, we assume that each RN can support a limited number of users. Then the problem to be studied is formulated as finding the deployment of a given number of RNs such that: (1) most MNs can be covered; (2) the network throughput can be maximized.

We first study the COverage-oriented Relay Placement (CORP) problem of deploying a set of M RNs to cover a maximum number of MNs. As an initial setup, we

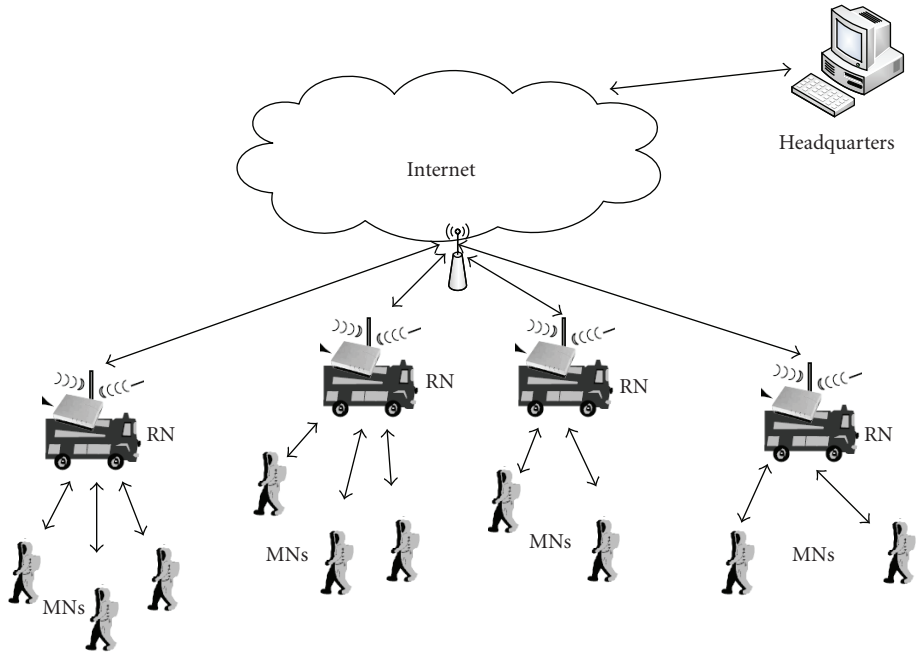

Figure 1: A realistic scenario of DAWN.

consider the subproblem of Relay Assignment for COverage-oriented Relay Placement (RA-CORP) which is, for any given RNs' placement, to obtain the optimal associations between RNs and MNs using maximal matching method. Secondly, the Greedy Incremental COverage (GICO) algorithm is proposed to iteratively find the optimal location for the RN, one at each time. Thirdly, we put forward the constrained exhaustive search (CES) method to produce the optimal solution to the CORP problem as a benchmark for the GICO algorithm.

We also investigate the CApacity-oriented Relay Placement (CARP) problem to maximize the total throughput of DAWN. In this case, the Relay Assignment for CApacity-oriented Relay Placement (RA-CARP) can be formulated as the assignment problem and solved by the Hungarian method [2]. Subsequently, we propose the Greedy Incremental Capacity (GICA) algorithm to find the RNs' positions one by one. In comparison, the optimal placement of all RNs can be obtained by solving a complicated binary integer programming problem but at very high computational complexity.

The rest of this paper is organized as follows. In Section 2, related work on disaster area networks, mobility model, and base station placement in wireless networks is summarized. In Section 3, we describe the mobility model of MNs within the disaster area; Section 4 presents the problem formulation of maximizing coverage for DAWN; Section 5 presents the technical approaches to solve the CORP problem. In Section 6, we present the problem formulation of maximizing aggregate throughput for DAWN. Subsequently, Section 7 presents the technical approaches to solve the CARP problem; simulation results are given in Section 8, followed by conclusions in Section 9.

2. Related Work

2.1. Disaster Area Wireless Network. Recently, many kinds of wireless networks have been proposed to be applied to disaster area relief operations. In [3], Hiroaki et al. propose and evaluate a mobile ad hoc network system to pursue the location and personal information of victims in occurrence of disaster. In [4], Kanchanasut et al. describe an emergency communication network platform designed for collaborative simultaneous emergency response operations using a combination of mobile ad hoc networking and a satellite IP network operating with conventional terrestrial internet. In [5], Malan et al. introduce a wireless infrastructure intended for emergency medical care, integrating low-power, wireless vital sign sensors, and PC-class systems. In addition, Zussman and Segall propose to construct an ad hoc network of wireless smart badges in order to acquire information from trapped survivors [6]. Besides, a novel ballooned wireless mesh network [7] has been proposed for emergency information system. All these works either assume the majority network nodes are static or mention little about their mobility model. Therefore, they fail in constructing the disaster area communication system to accommodate dynamic node configurations.

2.2. Macroscopic Mobility Model. In the recent years, several different macroscopic mobility models have been proposed and used for performance evaluation of networks. The fluid mobility model [8–10] conceptualizes traffic flow of users as the flow of a fluid, which models mobility in terms of the mean number of users crossing the boundary of a given area. Derived from transportation theory, these models give an aggregated description of the movement of several users,

ranging from street scale and city scale [11–13] to national and international scales [12, 14]. Furthermore, two different event-driven role-based mobility models are designed for disaster area relief applications [15, 16]. However, these two models only apply in small area with specific disaster sites.

2.3. Base Station Placement. There have been extensive researches dedicated to base station placement problem in wireless sensor networks. In [17], a multiobjective metric is proposed for placing multiple base stations at the optimal positions in wireless sensor networks, including coverage, fault tolerance, energy consumption, and network delay. In [18], Shi and Hou propose a (1-ξ) optimal approximation algorithm to place base station so that the network lifetime could be maximized. In [19], a polynomial time heuristic is proposed for optimal base station selection within a wireless sensor network. In [20], Pan et al. study base station placement problem to maximize network lifetime. Most of existing base station placement schemes are designed for wireless networks with nodes at specific positions. Therefore, they are not suitable for the proposed mobile scenarios.

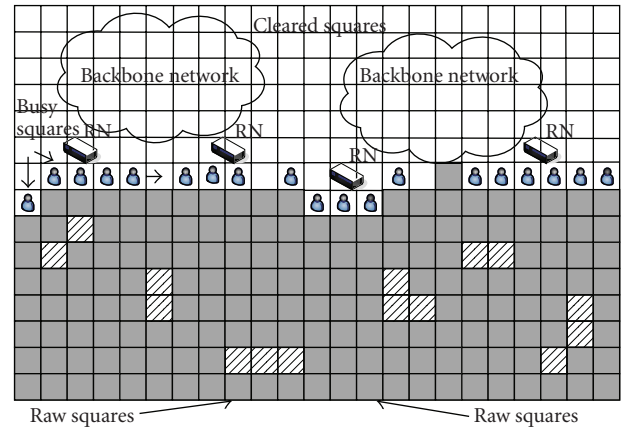

Figure 2: A realistic scenario of DAWN in the middle of the disaster area relief process. The squares with head portraits denote busy squares. White squares denote cleared squares. Dark squares denote disaster area yet to clear. Stripe squares represent unreachable spots within the disaster area.

3. System Modeling and Applications

3.1. Mobility Model. As shown in Figure 2, we discretize the entire disaster area into squares, each square with a Catastrophic Intensity (CI) value to indicate the severity of damage. The squares that are yet to be cleared are called *raw squares*. Those working-in-progress squares are also termed as *busy squares*. Both raw squares and busy squares are considered as *uncleared squares*. A square is said to be cleared if the CI value is reduced to zero. Faced with the mission of relieving such a large-scale disaster area, first responders ought to start from places near the boundary of the disaster area. The first responders do not stop working in the square until it is cleared. When first responders finish clearing a square, they split up and enter the adjacent uncleared squares. More specifically, the diversification is determined by the CI values and the current workforce in the neighboring squares. If obstacles and unreachable spots exist in the disaster area, as the stripe squares in Figure 2, first responders will make a detour according to our mobility model. As the first responders move deeper and broader spatially, they can finally clear the entire disaster area. The details of the mobility model can be referred to our prior work [1].

3.2. Network Model. We consider a set of MNs moving within the disaster area following the mobility model described previously and assume that a fixed number of RNs are ready for deploying to connect all MNs to the backbone network. We assume that all MNs have small transmission range r. The transmission region of an MN is defined as the area in which all points are within distance r from the MN. The ith MN n_i can communicate bi-directionally with the jth RN r_j if the distance between them $d(n_i, r_j) \leq r$. In other words, n_i is said to be covered by r_j if r_j is within the transmission region of n_i. RNs are able to communicate with each other without distance constraints and they form the backbone network. We assume that the relay stations can be installed on vehicles and can quickly move to any locations in the disaster area. We assume each MN occupies one orthogonal channel associated with an RN for at least one time unit to communicate bi-directionally. Since the RN has a limited bandwidth, each RN can only support a certain number of MNs. As a note, no interference issues are considered in our network model due to abundant unoccupied spectrum in the disaster area.

4. Maximizing Node Coverage: Problem Formulation

We first provide the notation used in this section. Let $V_{i,j}$ denote the set of four vertices of square $s_{i,j}$. C_k denotes the disk centering at r_k with radius as r. A spot p is said to be covered by C_k if $d(p, r_k) \leq r$, denoted as $p \in C_k$. A polygon G is said to be covered by C_k if for any point p within G, $d(p, r_k) \leq r$, denoted as $G \subset C_k$.

For the CORP problem, RNs should be placed at positions to connect the maximum number of MNs. As MNs follow a macroscopic mobility model, we choose to cover the active (busy) squares instead of tracking the individual MNs. In other words, if a busy square is covered, then all MNs within the square are connected. We now claim Theorem 1 to show that a square can be covered by a circle if and only if its four vertices are within that circle.

Theorem 1 (covering a polygon). *Assume a polygon $G = (V, E)$, where V and E denote the set of vertices and edges, respectively. If for all vertex $v_i \in V$, $d(v_i, r_k) \leq r$, then $G \subset C_k$.*

Proof. First of all, we need to acknowledge the fact that if $d(v_i, r_k) \leq r$, $d(v_j, r_k) \leq r$, then for all $p \in e(v_i, v_j)(e(v_i, v_j)$ denotes the edge connecting v_i and v_j), $d(p, r_k) \leq r$ (it is obviously true since the edge is fully contained in one circle if the two terminals are within the same circle). For

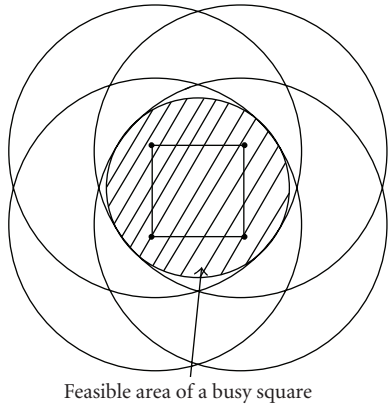

Figure 3: The feasible area to place the RN to cover one busy square. The 4 circles demarcate one region around the square, which can be approximated using a circle, shown as the shadow area.

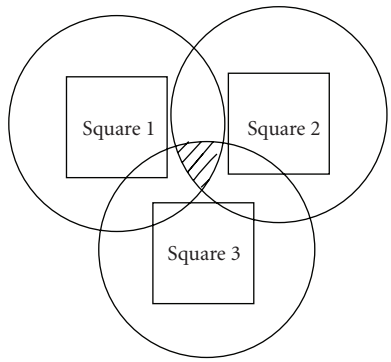

Figure 4: An example of three feasible circles mutually intersected, representing, respectively, as the round area with skew strips, horizontal strips, and points. The overlap area of the three circles in the middle represents the placement region where one RN can cover the three squares.

all $p \in G$, we have $p \in e(p_1, p_2)$, where $p_1 \in e(v_{m1}, v_{n1})$ and $p_2 \in e(v_{m2}, v_{n2})$. Since for all $v_i \in V$, $d(v_i, r_k) \le r$, then $d(p_1, r_k) \le r$ and $d(p_2, r_k) \le r$. As a result, $d(p, r_k) \le r$, and $G \subset C_k$. □

Based on Theorem 1, the region where one RN should be placed to cover one busy square approximates to a circle (shown as Figure 3), which is defined as the *feasible circle* of each square. For every busy square in the DAWN, each has a corresponding feasible circle. These feasible circles may overlap each other and the intersected areas are referred as *shared regions*. As shown in Figure 4, three feasible circles are intersected and an RN placed in the shared region (shaded area) can cover all 3 squares at the same time. In a DAWN, these shared regions form a candidate set for RN placement. In this paper, our analysis and simulations are derived directly based on the concept of shared regions, instead of using traditional Cartesian coordinates.

The CORP problem is defined as follows. Given a set of busy squares, in which each contains some MNs inside with transmission range r, and M RNs each with capability C, find the optimal placement of the RNs, such that the maximum number of MNs is covered.

5. Maximizing Node Coverage: Technical Approaches

In this section, we first present a maximal matching method to solve the RA-CORP problem if the RNs' positions are known. Secondly, we propose the GICO and CES algorithms to tackle the CORP problem. In addition, we conduct complexity analysis for both algorithms.

5.1. Relay Assignment for Fixed RN Positions (RA-CORP). The RA-CORP problem tries to find the optimal association between MNs and RNs. We use a bipartite graph to represent the RA-CORP problem, and then use a sparse matrix-based algorithm to find the maximum-sized matching between the MNs and RNs.

Definition 1. Denote the feasible circle of the jth busy square b_j as f_j. Assume $f_{i_1}, f_{i_2}, \ldots, f_{i_{l_i}}$ have some area overlap, then the intersection area is defined as a *shared region* that only MNs within busy squares $b_{i_k}, (1 \le k \le l_i)$ can access, denoted as $sr(f_{i_1}, f_{i_2}, \ldots, f_{i_{l_i}})$, or simply as sr_i.

At any time, MNs are distributed within a set of busy squares. The feasible circles of these busy squares intersect and yield a set of shared regions $\mathcal{SR} = \{sr(f_{i_1}, f_{i_2}, \ldots, f_{i_{l_i}}), 1 \le i \le K_{CA}\}$, where K_{CA} denotes the cardinality of the set $\mathcal{SR}$. A fixed number of RNs $\{r_1, r_2, \ldots, r_M\}$ are deployed at $sr(f_{j_1}, f_{j_2}, \ldots, f_{j_{l_j}})$, $1 \le j \le M$. Each RN can support at most C MNs within the squares covered by the RNs. Then the RA-CORP problem is formulated as

$$\begin{aligned} &\max \sum_{i=1}^{N}\sum_{j=1}^{M} x_{ij}, \\ &\text{s.t.} \quad x_{ij} \in \{0,1\}, \quad \forall i, j, \\ &\sum_{j \in H_i} x_{ij} \le 1, \quad \forall i, \\ &\sum_{i \in Q_j} x_{ij} \le C, \quad \forall j, \end{aligned} \tag{1}$$

where $x_{ij} = 1$ denotes that n_i is connected with r_j and 0 otherwise. H_i denotes the set of RNs that cover n_i. Q_j denotes the set of MNs that are covered by r_j. The second constraint demands that each MN can at most connect to one RN. The third constraint shows that at most C MNs can connect to one RN.

Given MNs placed within busy squares, and RNs deployed in some shared regions, the bipartite graph can be generated as in Figure 5, where N denotes the number of MNs. We prove that the maximal matching problem within a bipartite graph shown as Figure 5 is tantamount to the RA-CORP problem. In Figure 5, each MN can be assigned to any subband of an RN that covers the busy square where the MN

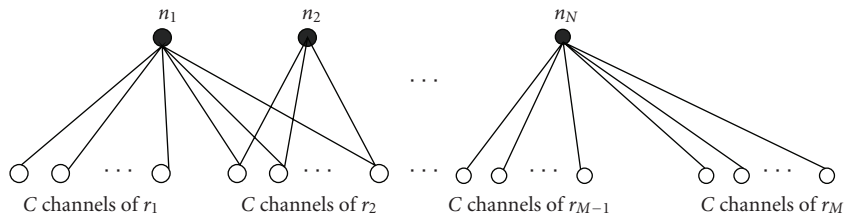

Figure 5: The bipartite graph example showing the association relationship between MNs and RNs.

is. Each line in Figure 5 shows that the corresponding MN can be connected to the RN with one channel. As each node of the bipartite graph can only be incident on one line, this bipartite graph correctly satisfies the second constraint in (1). Moreover, this bipartite graph extends each RN by C times to obtain the matchings between MNs and channels of RNs; this transformation successfully captures the third constraint in (1). Therefore, the RA-CORP problem is equivalent to the maximal-matching problem in a bipartite graph as shown in Figure 5.

In this paper, we use a sparse matrix-based approach [21] to find the maximal matching between MNs and channels of RNs for each RN. This approach yields the optimal solution. The complexity of finding the maximal matching within a bipartite graph is $O(M \times N^2)$.

5.2. Relay Placement for Optimal Coverage (CORP). We first claim Theorem 2 about complexity of the CORP problem.

Theorem 2. *The CORP problem is NP-complete.*

Proof. See Appendix A. □

Then we perform aggregation for all shared regions to reduce the solution space. Since the CORP problem is NP-complete, we introduce a heuristic approach GICO to solve the problem. To measure the performance of GICO, we also give the optimal solution by employing the CES algorithm.

5.2.1. Aggregation. The aggregation procedure aims to reduce the cardinality of the set of shared regions, thus greatly reduces the solution space. Given a set of shared regions $\mathcal{SR}$, the aggregation proceeds as in Algorithm 1. We say $sr(f_{i_1}, f_{i_2}, \ldots, f_{i_{l_i}})$ belongs to $sr(f_{j_1}, f_{j_2}, \ldots, f_{j_{l_j}})$ or $sr(f_{j_1}, f_{j_2}, \ldots, f_{j_{l_j}})$ contains $sr(f_{i_1}, f_{i_2}, \ldots, f_{i_{l_i}})$ if $\{i_1, i_2, \ldots, i_{l_i}\} \subseteq \{j_1, j_2, \ldots, j_{l_j}\}$. Let $\mathcal{SR}$ and $\overline{\mathcal{SR}}$ denote the set of all shared regions, and reduced set of shared regions, respectively. $|\overline{\mathcal{SR}}|$ denotes the cardinality of the set $\overline{\mathcal{SR}}$.

The procedure reduces the cardinality of the set of shared regions by removing those that are contained by others. The procedure reduces the solution space without losing any coverage options. The reason is that RNs placed in sr_i that contains sr_j can cover busy squares $\{b_{j_1}, b_{j_2}, \ldots, b_{j_{l_j}}\}$. Therefore, the set $\overline{\mathcal{SR}}$ can contain all shared regions but with the minimal cardinality.

5.2.2. Greedy Incremental Coverage (GICO). The GICO algorithm is based on the following idea. Although it is not computationally feasible to perform an exhaustive search for placing M RNs simultaneously, it is possible to choose an optimal position to place one RN at a time. When the RN is placed at each shared region, the optimal relay assignment can be obtained by utilizing the maximal matching method. The best shared region for placing one node can be found by exhaustively searching all shared regions in $\overline{\mathcal{SR}}$. Once the location for this RN is fixed, the next RN can be placed following the same procedure. It should be noted that when placing next RN, those previously placed RNs should be jointly considered for relay assignment in order to compute the coverage values. In this approach, the RNs are placed one by one until all M RNs are deployed in the set $\widehat{\mathcal{SR}}$.

```
Aggregation(SR)
1   SR̄ ← sr_1;
2   for i=2 to K_CA
3      sign=0;
4      for j=1 to |SR̄|
5         if sr_j belongs to sr_i
6            remove sr_j from SR̄;
7            sign=1;
8            end if;
9         if sr_i belongs to sr_j
10           sign=2;
11           break;
12        end if;
13     end for;
14  if sign==0 or sign==1
15     add sr_i to SR̄;
16     end if;
17  end for;
18  return SR̄;
```

Algorithm 1: Aggregation procedure.

As listed in Algorithm 2, GICO works as follows. $\widehat{\mathcal{SR}}$ represents the shared regions that have been chosen to place RNs. K_{CO} denotes the cardinality of $\overline{\mathcal{SR}}$. It is possible that $\widehat{\mathcal{SR}}$ contains multiple same shared regions, which means that multiple RNs should be placed in that shared region. At line 4, each shared region in the set $\overline{\mathcal{SR}}$ is added into the current set $\widehat{\mathcal{SR}}$ and the set $\widetilde{\mathcal{SR}}$ is obtained. The procedure at line 5 calculates and stores the maximal matching based on RNs' deployment according to the current $\widetilde{SR}$. **RA-CORP**$(\widetilde{\mathcal{SR}})$ denotes the calculated optimal maximal matching while $\widetilde{\mathcal{SR}}$ denotes the set of shared regions that

GICO ($\overline{\mathcal{SR}}$)
1 $\widehat{\mathcal{SR}} \leftarrow \emptyset$;
2 **for** i=1 to M
3 **for** j=1 to K_{CO}
4 $\widehat{\mathcal{SR}} \leftarrow \widehat{\mathcal{SR}} + \overline{\mathcal{S}}\,\overline{\mathcal{R}}_j$
5 $value_j \leftarrow$**RA-CORP**($\widetilde{\mathcal{S}}\,\widetilde{\mathcal{R}}$)
6 **end for**;
7 [maximum, index]=**Max**(value);
8 $\widehat{\mathcal{SR}} \leftarrow \widehat{\mathcal{SR}} + \overline{\mathcal{S}}\,\overline{\mathcal{R}}_{\text{index}}$;
9 **end for**;
10 **return** $\widehat{\mathcal{SR}}$;

Algorithm 2: GICO.

each contains one RN. After executing the procedure of lines 4 and 5 for K_{CO} times, the best next shared region to place one RN is found (line 7) and added to the set $\widehat{\mathcal{SR}}$ (line 8). Therefore, after greedily choosing RN placement one by one for M times, we can finally obtain the solution.

5.2.3. Constrained Exhaustive Search (CES). In order to obtain the optimal solution as a benchmark for our GICO algorithm, we need to search all possible combinations of the shared regions. However, even after employing the aggregation procedure to reduce the size of solution space, the complexity for searching the optimal solution could still be as high as $(K_{CO})^M$. Therefore, we resort to devising the CES algorithm to further reduce the solution space by adding one constraint to the combinations of shared regions. The constraint is that for each set of M RN placements, each RN should cover at least one MN based on the RA-CORP results. In particular, the number of RNs placed in one shared region times RNs' capability should not exceed the total number of MNs in those busy squares that are covered by the RNs by more than C, shown as

$$N_{RN}^{i} \times C \le \sum_{j=i_1}^{i_{l_i}} N_{MN}^{j} + C, \tag{2}$$

where N_{RN}^{i} denotes the number of RNs placed at sr_i and N_{MN}^{j} denotes the number of MNs in the busy square b_j.

5.3. Complexity Analysis. We first discuss the complexity of the aggregation procedure. Based on Algorithm 1, the procedure between line 5 to line 12 is iterated $(K_{CA}-1)\times K_{CO}$ times, and the procedure between line 14 to line 16 is iterated $K_{CA}-1$ times. As neither K_{CO} nor K_{CA} is influenced by N, the complexity for the aggregation procedure is $O(1)$.

Secondly, we analyze the complexity of GICO. Based on Algorithm 2, the complexity of the GICO algorithm is $O(M^2N^2K_{CO})$, because the procedure from line 4 to line 5 is iterated MK_{CO} times, and the worst case complexity for the maximal matching method is $O(MN^2)$.

For CES, the complexity analysis is more complicated. According to the constraint in (2), each shared region cannot host more than a limited number of RNs. Therefore, we assume on average each shared region can host ϵ ($1 \le \epsilon \le M$) RNs, as shown in

$$\epsilon = \frac{1}{K_{CO}} \sum_{i=1}^{K_{CO}} \left\lceil \frac{\sum_{j=i_1}^{j=i_{l_i}} N_{MN}^{j}}{C} \right\rceil. \tag{3}$$

In other words, the list of shared regions can be extended to a longer one with length ϵK_{CO}, on which each shared region can host at most one RN. As the worst case complexity for the maximal matching method is $O(MN^2)$, the computation complexity for CES can be stated as $O(MN^2\binom{\epsilon K_{CO}}{M})$. Now we claim that the complexity of the CES algorithm is higher than GICO, as shown in Theorem 3.

Theorem 3 (complexity of GICO and CES). *The complexity of the GICO algorithm is lower than the complexity of the CES algorithm.*

Proof. As already explained, the complexity of GICO is $O(M^2N^2K_{CO})$ while the complexity for CES is $O(MN^2\binom{\epsilon K_{CO}}{M})$. We can tell that K_{CO} has little relation with N, while M is roughly linearly related with N, that is, $M = \lambda N (1/N \le \lambda \le 1)$, because the more MNs, the more channels are required to access them to the backbone network. Then we can develop the ultimate form for the complexity of GICO as

$$O(M^2N^2K_{CO}) = O(K_{CO}\lambda^2 N^4) = O(N^4). \tag{4}$$

By substituting ϵ in (5) with (3), the ultimate form for the complexity of CES is developed as

$$\begin{aligned} &O\left(MN^2\binom{\epsilon K_{CO}}{M}\right) \\ &= O\left(MN^2 \frac{(\epsilon K_{CO})!}{(\epsilon K_{CO}-M)!M!}\right) \\ &= O\left(\lambda N^3 \left(\left(\frac{\epsilon K_{CO}}{M}\right)^{\lambda}\right)^{N}\right) \\ &= O\left(N^3 \left(\left(\frac{1}{M}\sum_{i=1}^{K_{CO}} \left\lceil \frac{\sum_{j=i_1}^{j=i_{l_i}} N_{MN}^{j}}{C} \right\rceil\right)^{\lambda}\right)^{N}\right). \end{aligned} \tag{5}$$

Obviously, the term $(1/M)\sum_{i=1}^{K_{CO}} \lceil \sum_{j=i_1}^{j=i_{l_i}} N_{MN}^{j}/C \rceil > 1$. Therefore, the complexity for GICO is less than the complexity for CES. □

6. Maximizing Aggregate Throughput: Problem Formulation

In Section 4, we formulate the CORP problem, which is aimed to maximize the number of MNs that can be connected to the backbone network. However, the objective of the CORP problem does not address the quality of service

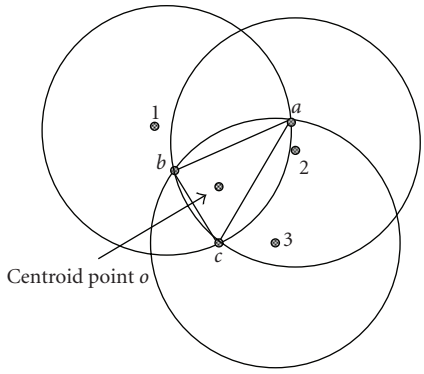

Figure 6: An example to describe the centroid point of a shared region. The intersection points of the shared region sr_{f_1,f_2,f_3} are points a, b, and c. Then the centroid point o of the triangle abc is regarded as the position of any RN that is placed within SR_{f_1,f_2,f_3}.

(QoS) requirements of individual links. In other words, the deployment of RNs has to consider not only the coverage but also the QoS performance with intelligent channel allocation. Therefore, we put forward the CARP problem in the interest of enhancing the QoS performance of DAWN.

To measure the throughput of individual links, we ought to set the positions of RNs as exact Cartesian coordinates. In particular, instead of defining the position of an RN as a region, we specify its position as the centroid point of the polygon, whose vertices are the intersection points of the arcs of a region in counterclockwise order. An example is shown in Figure 6. Let us denote the coordinates of the intersection points of sr_i as $\{(x_p, y_p), 1 \le p \le i_{l_i}\}$, the coordinates of the centroid point as (x_{o_i}, y_{o_i}), where o_i denotes the centroid point of sr_i. Then the coordinates of the centroid point is calculated as

$$\begin{aligned} x_{o_i} &= \frac{1}{6A}\left[\sum_{p=1}^{i_{l_i}-1}\left(x_p + x_{p+1}\right)\left(x_p y_{p+1} - x_{p+1} y_p\right)\right. \\ &\qquad \left. + \left(x_{i_{l_i}} + x_1\right)\left(x_{i_{l_i}} y_1 - x_1 y_{i_{l_i}}\right)\right], \\ y_{o_i} &= \frac{1}{6A}\left[\sum_{p=1}^{i_{l_i}-1}\left(y_p + y_{p+1}\right)\left(y_p x_{p+1} - y_{p+1} x_p\right)\right. \\ &\qquad \left. + \left(y_{i_{l_i}} + y_1\right)\left(y_{i_{l_i}} x_1 - y_1 x_{i_{l_i}}\right)\right], \end{aligned} \tag{6}$$

where A denotes the area of the polygon formed by connecting the intersection points in a counterclockwise order, which can be calculated using

$$A = \frac{1}{2}\left[\left(\sum_{p=1}^{i_{l_i}-1} x_p y_{p+1} - x_{p+1} y_p\right) + \left(x_{i_{l_i}} y_1 - x_1 y_{i_{l_i}}\right)\right]. \tag{7}$$

Based on Shannon formula, the channel capacity of a link can be expressed as (8) using path loss model

$$F = W \times \log_2\left(1 + \frac{P_t G_t G_r (w/4\pi)^2}{d^{\alpha} P_{\text{noise}}}\right), \tag{8}$$

where F denotes the capacity of the channel, W denotes the bandwidth of the channel, d denotes the distance between the transmitter and receiver of the link, α denotes the path loss coefficient, P_t denotes the transmit power, P_{noise} denotes the noise power, G_t and G_r are the transmitter and receiver antenna gains, respectively, $w = c/f$ denotes the wavelength of the transmitted signal, f denotes the frequency of the transmitted signal, c is the velocity of radio-wave propagation in free space, which is equal to the speed of light.

Since MNs follow the macroscopic mobility model, we resort to developing the two-dimensional integral (9) to compute the throughput of the link between an MN and its assigned RN. In (9), (x_i, y_i) denotes the coordinates of the left downward vertex of the ith busy square b_i. e_{ik} denotes the throughput of the link between one MN in b_i and one RN placed at o_k. L denotes the side length of each square

$$e_{ik} = \begin{cases} \dfrac{1}{L^2}\displaystyle\int_{x_i}^{x_i+L}\int_{y_i}^{y_i+L} W \\ \qquad \times \log_2\left(1 + \dfrac{P_t G_t G_r (w/4\pi)^2}{d(o_k,(x,y))^{\alpha} P_{\text{noise}}}\right) dx dy : \\ \qquad\qquad i \in \{k_1, k_2, \ldots, k_{l_k}\}, \\ 0 : \qquad\qquad i \notin \{k_1, k_2, \ldots, k_{l_k}\}. \end{cases} \tag{9}$$

The CARP problem is formulated as follows. Given N MNs each with transmission range r that are distributed within a set of busy squares and M RNs each with capability C, find the optimal positions for the RNs such that the aggregated throughput of all established links between MNs and RNs are maximized.

7. Maximizing Aggregate Throughput: Technical Approaches

In this section, we investigate the CARP problem of deploying a set of RNs to maximize the total throughput of DAWN. We first consider the optimal relay assignment for fixed RN positions, which can be solved using the Hungarian method. On this basis, we propose the GICA approach to tackle the CARP problem. In addition, since the CARP problem falls into a binary integer programming formulation, the branch and bound algorithm [22] is adopted to produce the optimal solution as the benchmark for the GICA approach.

7.1. Relay Assignment for Fixed RN Positions (RA-CARP). At any time, MNs are distributed within a set of busy squares. The feasible circles of these busy squares intersect and yield a set of shared regions $\mathcal{SR} = \{sr(f_{i_1}, f_{i_2}, \ldots, f_{i_{l_i}}), 1 \le i \le K_{CA}\}$. A fixed number of RNs $\{r_1, r_2, \ldots, r_M\}$ are deployed at the set

of centroid points $\{o_{u_j}\}, 1 \le j \le M$. Each RN can support at most C MNs to access the network in the squares that it covers. Now the RA-CARP problem is formulated as

$$\begin{aligned} &\max \sum_{i=1}^{N}\sum_{j=1}^{M} e_{a(i)k(j)}x_{ij}, \\ &\text{s.t.} \quad x_{ij} \in \{0,1\}, \quad \forall i,j, \\ &\sum_{j\in H_i} x_{ij} \le 1, \quad \forall i, \\ &\sum_{i\in Q_j} x_{ij} \le C, \quad \forall j, \end{aligned} \tag{10}$$

where $x_{ij} = 1$ denotes that n_i is connected with r_j and 0 otherwise; $a(i)$ denotes the index of the busy square where n_i is. $k(j)$ denotes the index of the shared region where r_j is placed. The second constraint denotes that each MN can at most connect to one RN. The third constraint shows that at most C MNs can connect to one RN.

Given MNs placed within busy squares and RNs deployed in some shared regions, the bipartite graph can be generated as in Figure 5. It can be seen that for each MN-RN pair, there are C edges each with a weight equal to the capacity value of the corresponding link. Note that for those pairs that the RN does not cover the MN, the edges are assigned weights equal to 0. We now can generate a gain matrix $\mathbf{g}$ shown as

$$\mathbf{g} = \begin{Bmatrix} g_{11} & g_{12} & \cdots & g_{1J} \\ g_{21} & g_{22} & \cdots & g_{2J} \\ : & : & & : \\ : & : & & : \\ g_{N1} & g_{N2} & \cdots & g_{NJ} \end{Bmatrix}, \tag{11}$$

where $J = M \times C$ and $g_{ij} = e_{a(i),k(\lceil j/C \rceil)}$. We now present the Hungarian method [2] as follows.

Step 1. If $\mathbf{g}$ is not a square matrix, we have to augment $\mathbf{g}$ into a square matrix by padding rows or columns with all zeros.

Step 2. Multiply the matrix $\mathbf{g}$ by -1.

Step 3. Subtract the minimum value of each row from row entries.

Step 4. Subtract the minimum value of each column from column entries.

Step 5. Select rows and columns across which you draw lines, such that all zeros are covered and that no more lines have been drawn than necessary.

Step 6. If the number of lines equals the number of rows, choose a combination of zero elements from the modified gain matrix such that the position of each chosen element is incident on a unique row and column. Then the optimal assignment result consists of the RN-MN pairs as represented by the chosen elements in the modified gain matrix. If the number of lines is less than the number of rows, go to Step 7.

```
GICA(Ō)
1   Ô ← ∅;
2   for i=1 to M
3       for j=1 to K_CA
4           Õ ← Ô + O_j
5           value_j ←RA-CARP(Õ)
6       end for;
7       [maximum, index]=Max(value);
8       Ô ← Ô + O_index;
9   end for;
10  return Ô;
```

Algorithm 3: GICA.

Step 7. Find the smallest element which is not covered by any of the lines. Then subtract it from each entry which is not covered by the lines and add it to each entry which is at the intersection of a vertical and horizontal line. Go back to Step 5.

7.2. Relay Placement for Maximal Aggregate Throughput (CARP). We claim Theorem 4 about complexity of the CARP problem.

Theorem 4. *The CARP problem is NP-complete.*

Proof. See Appendix B. □

Since the CARP problem is NP-complete, we introduce a heuristic approach GICA to solve the problem. To measure the performance of GICA, we also present the optimal method for the CARP problem.

7.2.1. Greedy Incremental Capacity (GICA). According to Algorithm 3, the algorithm works as follows. $\hat{\mathcal{O}}$ denotes the set of centroid points that have been chosen to place RNs. $\mathcal{O}$ denotes the set of centroid points of all shared regions. $\hat{\mathcal{O}}$ denotes the set of centroid points that have been chosen. $\tilde{\mathcal{O}}$ denotes a current set of centroid points with each hosting one RN. At line 4, each centroid point in $\mathcal{O}$ is added to $\hat{\mathcal{O}}$ and the set $\tilde{\mathcal{O}}$ is obtained. The procedure at line 5 calculates and stores the total throughput yielded by the Hungarian method based on $\tilde{\mathcal{O}}$. **RA-CARP**$(\tilde{\mathcal{O}})$ denotes the calculated optimal association between MNs and RNs. After executing the procedure of lines 4 and 5 for K_{CA} times, the best next centroid point to place one RN is found (line 7) and added to $\hat{\mathcal{O}}$(line 8). Therefore, after greedily choosing centroid points one by one for M times, we can finally obtain the set of centroid points $\hat{\mathcal{O}}$ to place RNs.

7.2.2. Optimal Solution to CARP Problem. We show that the RA-CARP can be formulated as a binary integer programming problem when RNs are placed at fixed positions. Subsequently, the GICA method utilizes the Hungarian method to greedily place one RN at an iteration. Therefore, the solutions yielded by GICA cannot be guaranteed optimal

because the RN assignment and placement are considered separately. It would be natural to believe that only when we search all solution space can the optimal solution be produced.

Hereby we introduce two binary variables x_{ij} and y_{jk}. $x_{ij} = 1$ denotes that n_i is connected with r_j and 0 otherwise; $y_{jk} = 1$ denotes that r_j is placed at the centroid point of the kth shared region and 0 otherwise. Then we can jointly formulate the CARP problem as

$$\begin{aligned}
&\max \sum_{i=1}^{N}\sum_{j=1}^{M}\sum_{k=1}^{K_{CA}} e_{a(i)k} \times x_{ij} \times y_{jk},\\
&\text{s.t.} \quad x_{ij} \in \{0,1\}, \quad \forall i,j,\\
&\quad y_{jk} \in \{0,1\}, \quad \forall j,k,\\
&\quad \sum_{j=1}^{M} x_{ij} \le 1, \quad \forall i,\\
&\quad \sum_{i=1}^{N} x_{ij} \le C, \quad \forall j,\\
&\quad \sum_{k=1}^{K_{CA}} y_{jk} = 1, \quad \forall j,\\
&\quad \sum_{j=1}^{M}\sum_{k=1}^{K_{CA}} y_{jk} = M.
\end{aligned} \tag{12}$$

Since the objective term $e_{a(i)k} \times x_{ij} \times y_{jk}$ contains the product of two variables x_{ij} and y_{jk}, it is difficult to solve. According to [23], the product of multiple binary variables $x_1 x_2 \cdots x_t$ can be substituted by a new variable z with two constraints that ensure that $z = 0$ if there exists $i(1 \le i \le t), x_i = 0$, and $z = 1$ if for all $i(1 \le i \le t), x_i = 1$. Therefore, we transform (12) into a binary integer programming problem shown as

$$\begin{aligned}
&\max \sum_{i=1}^{N}\sum_{j=1}^{M}\sum_{k=1}^{K_{CA}} e_{a(i)k} \times z_{ijk},\\
&\text{s.t.} \quad z_{ijk} \in \{0,1\}, \quad \forall i,j,k,\\
&\quad x_{ij} + y_{jk} - z_{ijk} \le 1, \quad \forall i,j,k,\\
&\quad x_{ij} + y_{jk} \ge 2z_{ijk}, \quad \forall i,j,k,\\
&\quad x_{ij} \in \{0,1\}, \quad \forall i,j,\\
&\quad y_{jk} \in \{0,1\}, \quad \forall j,k,\\
&\quad \sum_{j=1}^{M} x_{ij} \le 1, \quad \forall i,\\
&\quad \sum_{i=1}^{N} x_{ij} \le C, \quad \forall j,\\
&\quad \sum_{k=1}^{K_{CA}} y_{jk} = 1, \quad \forall j,\\
&\quad \sum_{j=1}^{M}\sum_{k=1}^{K_{CA}} y_{jk} = M.
\end{aligned} \tag{13}$$

Now the CARP problem is formulated as a binary integer programming problem. We then utilize the branch and bound algorithm to solve it. The algorithm searches for an optimal solution by solving a series of LP-relaxation problems, in which the binary integer requirement on the variables x_{ij}^k is replaced by the weaker constraint $0 \le x_{ij}^k \le 1$. More details can be referred to [22].

7.3. Complexity Analysis. We first discuss the computation complexity of the Hungarian method to assign MNs when RNs are placed at fixed positions. According to [2], the complexity is $O(\max\{N, C \times M\}^4)$.

Then we analyze the complexity of the GICA algorithm. Let K_{CA} denote the number of shared regions. Based on Algorithm 3, as the procedure on lines 4 to 5 is iterated MK_{CA} times, the computation complexity of the GICA algorithm is $O(\sum_{j=1}^{M} K_{CA} \max\{N, C \times j\}^4) = O(N^5)$.

The optimal method to the CARP problem uses the branch and bound algorithm to solve a binary integer programming problem. As the number of binary variables is $MNK_{CA} + MN + MK_{CA}$, the worst case complexity for the optimal method is $O((2^{K_{CA}\lambda N + \lambda N + \lambda K_{CA}})^N)$. It is apparent that the complexity of the GICA algorithm is much lower than the optimal algorithm.

8. Simulation Results

In this section, we present the numerical results obtained from the simulation using high level programming language. For the CORP problem, we compare the performance of the GICO algorithm and the CES algorithm. For the CARP problem, we compare the performance of the GICA algorithm and the optimal algorithm. It is illustrated that the two greedy algorithms both merit close-to-optimal performance and low complexity.

8.1. Simulation Setup. We present the simulation results in a 10×10 square disaster area. The CI values of each square are initially set as 5 or randomly chosen in the interval [1 10] in Table 1. We implement two initial distributions of MNs: 40 MNs assemble at $s_{1,1}$ or evenly divided at 4 corners $s_{1,1}$, $s_{10,1}$, $s_{1,10}$, $s_{10,10}$. Thus we can obtain four different scenarios with each of the two distributions of CI values when MNs follow each of the two initial deployments. The bandwidth for each channel is 1 Mbps. The area of each square is $1000 \times 1000\,\text{m}^2$. Disaster relief efficiency coefficient is $\xi = 1$, which means each first responder can clear 1 unit of CI per unit time. The transmit power of MNs P_t is set to 1 watt. The transmitter and receiver antenna gains $G_t = G_r = 10$. The frequency is 2.4×10^9 Hz. The noise power P_{noise} is 1×10^{-8} watt. The path loss exponent is set as $\alpha = 2$. The transmission range r of MNs is set as 1500 meters.

8.2. Simulation Results for Maximal Coverage. We introduce *coverage percentage* as the measurement of coverage performance, which is defined as the ratio of the number of covered MNs to the total number of MNs working in the disaster area.

Table 1: The initial configuration of CI values of squares in disaster area. The CI values are randomly chosen between the interval [1 10].

Square index	1	2	3	4	5	6	7	8	9	10
1	2	10	10	5	9	2	5	10	8	10
2	7	1	9	10	7	8	8	4	7	2
3	8	1	3	1	1	9	7	4	10	1
4	5	4	8	8	2	5	5	7	8	8
5	3	7	7	2	2	5	10	4	6	3
6	8	3	6	7	9	10	6	2	2	3
7	9	3	9	3	10	4	2	3	7	5
8	4	9	6	6	10	3	8	8	4	6
9	1	1	6	8	10	2	6	5	1	4
10	2	8	4	6	2	7	3	7	7	8

Figure 7 shows the covering percentage of four scenarios for the entire disaster area relief process. It is clear that GICO performs very close to the optimal CES algorithm. In addition, results of all four scenarios share a similarity; the covering percentage is quite high during both initial and final periods (equal to 1), while lower during the middle of the disaster area relief process. The reason is that in the middle of the process, all the MNs are working in many widely distributed busy squares within the disaster area, thus the covering percentage is low due to limited covering range of RNs. On the other hand, in both initial and final periods, MNs are located in only a few spatially close squares, which renders covering the MNs an easy task as long as the channel resources are abundant. It is also worth pointing out that results from Figure 7(c) vibrate more dynamically than other 3 subfigures. This phenomenon shows that the number of busy squares is relatively small during the disaster area relief process if the first responder starts from one location and the CI values are random.

Next, in Figure 8, we look at the average covering percentage over the entire disaster area relief process for four scenarios when the capability of each RN changes. As can be observed, both algorithms yield better coverage performance if each RN can support more MNs. This is because more channel resources brought by RNs can accommodate more MNs. In addition, it is worth mentioning that as the capability of RNs is enlarged, less improvement is rendered for the covering percentage. The reason is that when one RN can cover more MNs, less uncovered MNs are left to boost the covering percentage in the future. In the end, it is clear that the GICO algorithm produces close-to-optimal solutions.

In Figure 9, we compare the performance of GICO and CES in terms of the average covering percentage over the entire disaster area relief process when the number of RNs changes. It is clearly shown that the GICO algorithm produces close-to-optimal solutions. As expected, in all four scenarios, both GICO and CES yield better performance in terms of average covering percentage as the number of RNs increases. This can be explained by the fact that more channel resources brought by RNs can accommodate more MNs. The coverage percentage asymptotically approaches 1 when the number of RNs becomes more than 6 for one starting location and 10 for 4 starting locations. By comparing the 4 subfigures, we can point out that the two curves corresponding with the scenarios that MNs start from 1 corner rises more sharply than the curves demonstrating scenarios that MNs start from 4 corners. The rationale is that during early periods, when MNs start from 4 corners, MNs disperse quickly to more squares than the case starting from a single location. Then limited RNs would produce better performance with MNs more crowded. Therefore, when RNs are very limited, it is preferable to start the MNs from 1 corner for coverage-oriented DAWN.

8.3. Simulation Results for Maximal Throughput. In Figure 10, we look at the average total throughput over the entire disaster area relief process for four scenarios when the number of RNs changes. As expected, it can be noted that both algorithms yield better performance in terms of total link throughput when the number of RNs increases, which is due to the fact that more RNs can accommodate more MNs or produce more reliable links. In addition, it is worth mentioning that as the capability of RNs increases, less improvement is rendered for the total link throughput. This is because when the capacity of channels is larger, less chances are given for those uncovered MNs or MNs with unreliable links to improve the total throughput. By comparing the 4 subfigures, we can see that when the capability of RNs is small, GICA produces better results for the scenarios that MNs start from 1 corner than that of all MNs starting from 4 corners. This is because during early periods, when MNs start from one corner, MNs expand less quickly to more squares than the scenarios that MNs start from 4 corners. Therefore, when the capability of RNs is very limited, it is preferable to start MNs from 1 corner for capacity-oriented DAWN, too. In the end, it is easily seen that the GICA algorithm produces close-to-optimal solutions.

Next, in Figure 11, we look at the average total throughput over the entire disaster area relief process when the capability of RNs changes. It can be noted that for four scenarios, both algorithms yield better performance in terms of total link throughput when each RN can support more

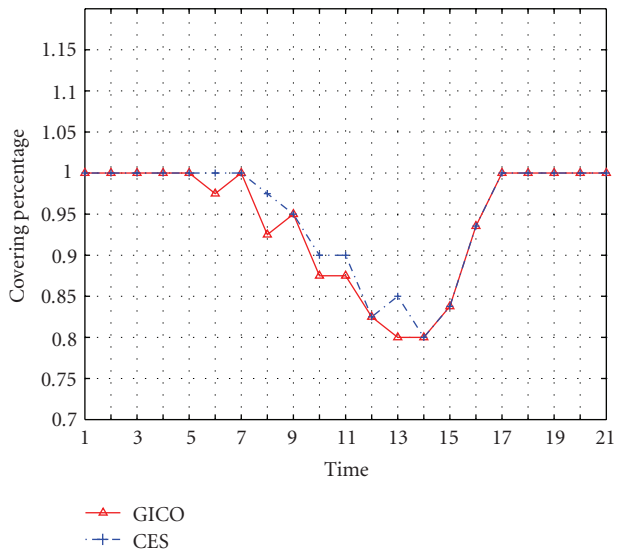

(a) At initial stage, 40 MNs are in $s_{1,1}$ at time 0, and CI values of all squares are 5

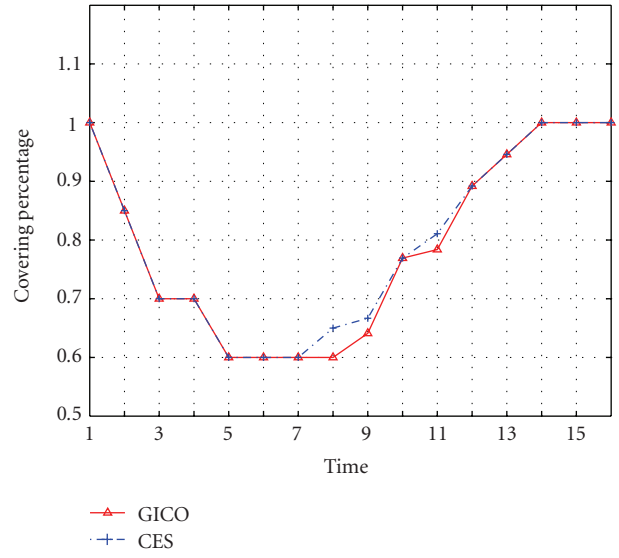

(b) At initial stage, 40 MNs are evenly deployed in $s_{1,1}$, $s_{1,10}$, $s_{10,1}$, $s_{10,10}$ at time 0, and CI values of all squares are 5

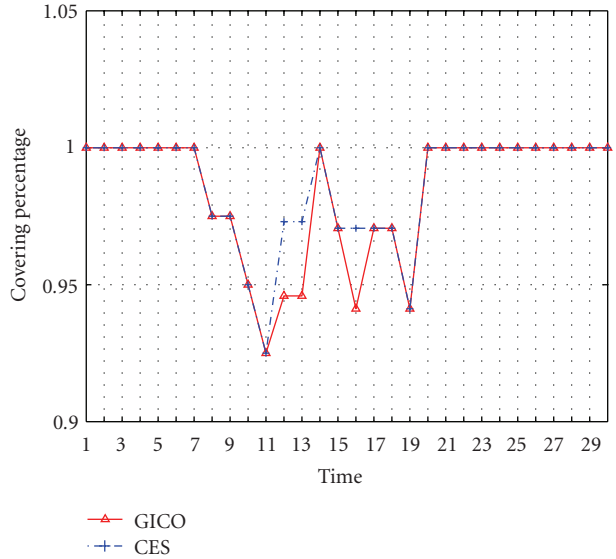

(c) At initial stage, 40 MNs are in $s_{1,1}$ at time 0, and CI values of all squares are randomly chosen between 1 and 10

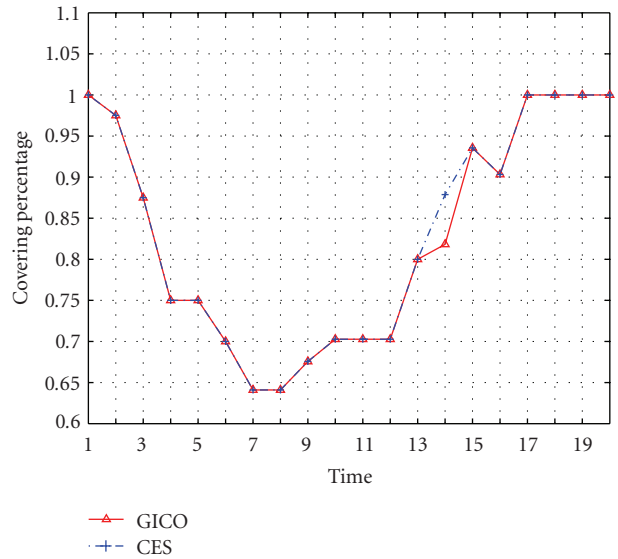

(d) At initial stage, 40 MNs are evenly deployed in $s_{1,1}$, $s_{1,10}$, $s_{10,1}$, $s_{10,10}$ at time 0. CI values of all squares are randomly chosen between 1 and 10

FIGURE 7: The covering percentage over the entire disaster area relief process in four scenarios. $r = 1.5\,L$, $C = 10$, $M = 5$.

MNs. The rationale behind is that more channel resources brought by RNs can accommodate more MNs or produce more reliable links. In addition, it can be observed that as the capability of RNs is enlarged, less improvement is rendered for total link throughput. This is because when one RN can cover more MNs, less uncovered MNs are left. By comparing the 4 subfigures, it can be found that although the algorithms yield similar results for 4 different scenarios when the capability of RNs is small, the throughput performance converges at a higher value as the capability of RNs increases for scenarios that MNs start from 1 corner than scenarios that MNs start from 4 corners. This phenomenon stems from the fact that when MNs start from 1 corner, a smaller average number of busy squares are generated over the disaster relief process. Even when the capability for RNs is high, the network throughput performance still suffers from wide distribution of the MNs for scenarios that MNs start from 4 corners. Therefore, it is preferable to start MNs from 1 corner for capacity-oriented DAWN regardless of the capability of RNs. In the end, as can be observed, the GICA algorithm produces close-to-optimal solutions.

9. Conclusion

In this paper, we study the dynamic deployment of mobile relays in DAWN to enable and improve the communications

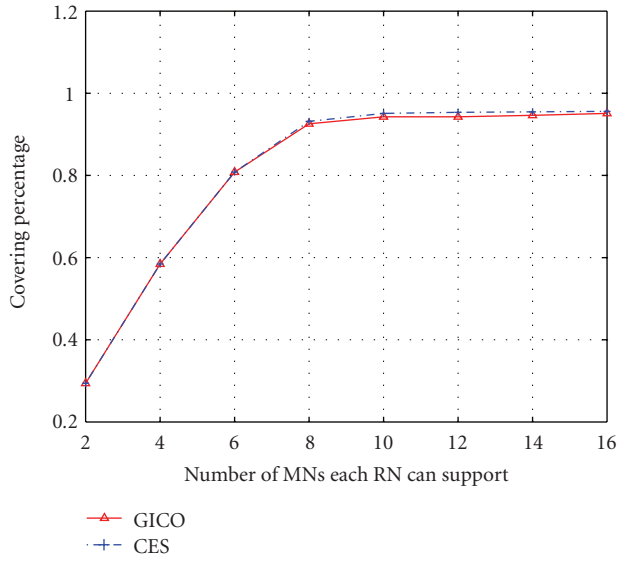

(a) At initial stage, 40 MNs are in $s_{1,1}$ at time 0, and CI values of all squares are 5

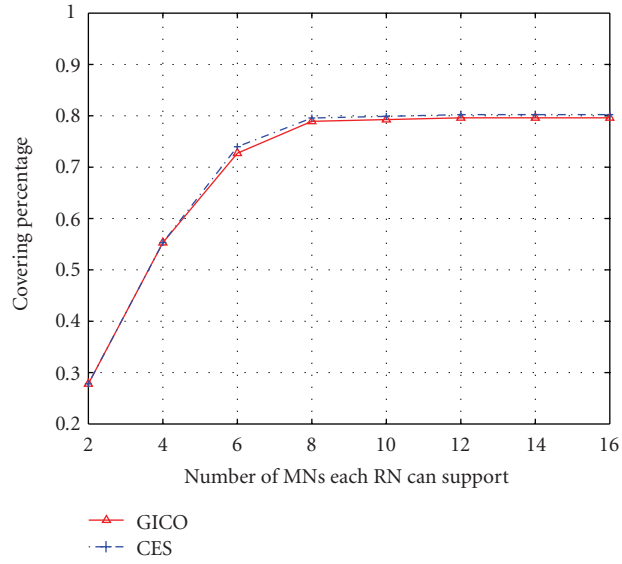

(b) At initial stage, 40 MNs are evenly deployed in $s_{1,1}$, $s_{1,10}$, $s_{10,1}$, $s_{10,10}$ at time 0, and CI values of all squares are 5

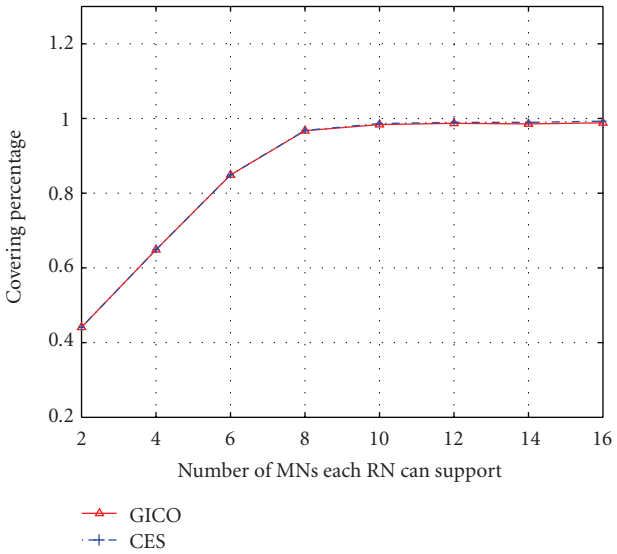

(c) At initial stage, 40 MNs are in $s_{1,1}$ at time 0, and CI values of all squares are randomly chosen between 1 and 10

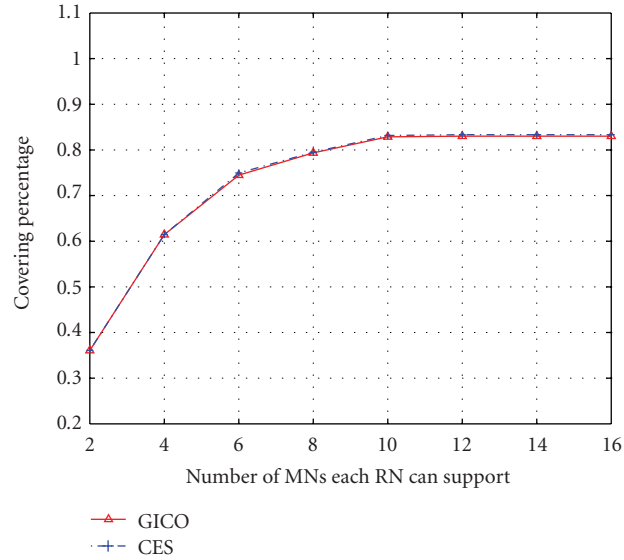

(d) At initial stage, 40 MNs are evenly deployed in $s_{1,1}$, $s_{1,10}$, $s_{10,1}$, $s_{10,10}$ at time 0. CI values of all squares are randomly chosen between 1 and 10

FIGURE 8: Average covering percentage over the entire relief process versus different capability of RNs in four scenarios. $r = 1.5\,L$, $M = 5$.

for the first responders during their operations. A mobility model is used to capture the movement pattern of the MNs and their communications to the RNs. Given a fixed number of relay nodes, the optimization problem is to determine the locations of the RNs as the MNs move in the disaster area nomadically. Two performance objectives, including maximal node coverage and maximal network capacity, are considered, respectively, in this study.

In the coverage problem (CORP), the performance objective is to place the RNs that can connect the maximum number of MNs in the network. As a preliminary step, we employ a maximal matching method to find the optimal relay node assignment for the static network scenario, that is, all RNs are fixed. Subsequently, we present the greedy incremental coverage algorithm (GICO) and the optimal constrained exhaustive search (CES) algorithms. The GICO algorithm is suboptimal but with significantly less computational complexity than the CES algorithm. The simulation results show that GICO algorithm can achieve close to optimal performance at different network setup and configurations.

In the capacity problem (CARP), the performance objective is to maximize the aggregated network throughput for all MNs in the DAWN. As an initial step, we first

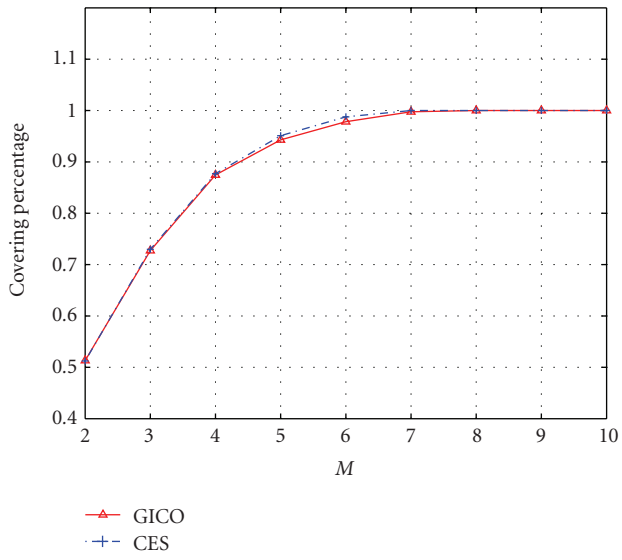

(a) At initial stage, 40 MNs are in $s_{1,1}$ at time 0, and CI values of all squares are 5

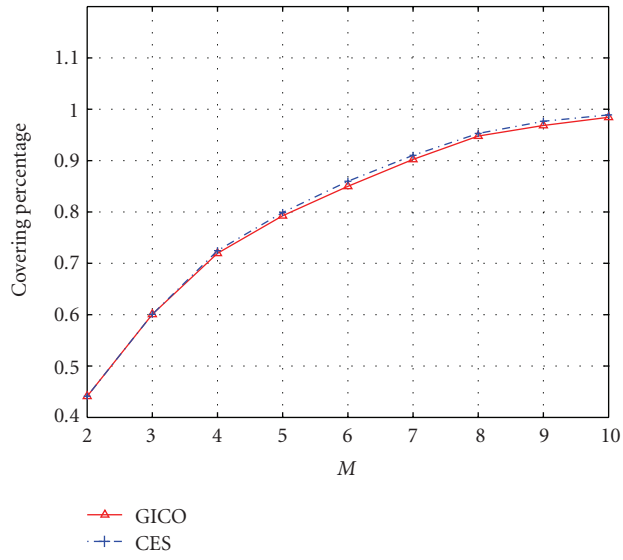

(b) At initial stage, 40 MNs are evenly deployed in $s_{1,1}$, $s_{1,10}$, $s_{10,1}$, $s_{10,10}$ at time 0, and CI values of all squares are 5

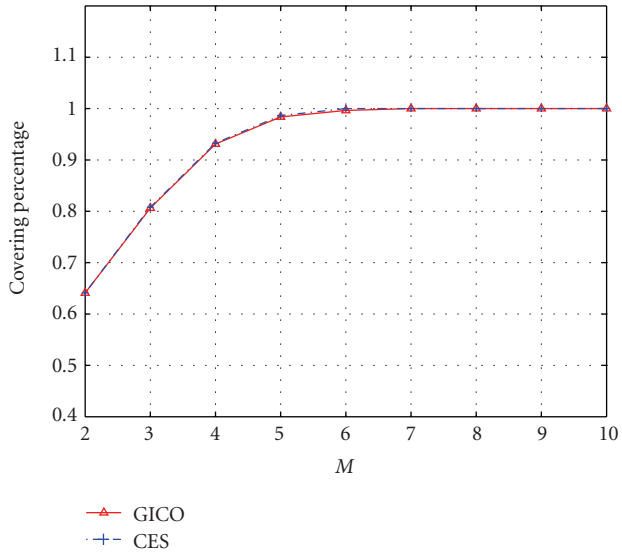

(c) At initial stage, 40 MNs are in $s_{1,1}$ at time 0, and CI values of all squares are randomly chosen between 1 and 10

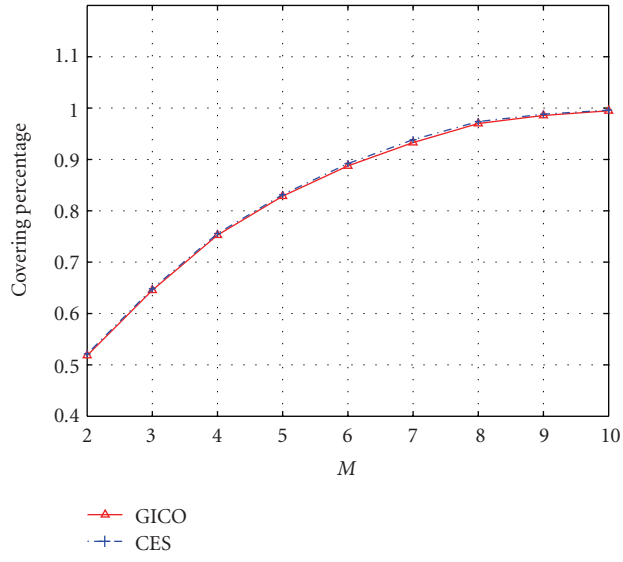

(d) At initial stage, 40 MNs are evenly deployed in $s_{1,1}$, $s_{1,10}$, $s_{10,1}$, $s_{10,10}$ at time 0. CI values of all squares are randomly chosen between 1 and 10

FIGURE 9: Average covering percentage over the entire relief process versus different number of RNs in four scenarios. $r = 1.5L$, $C = 10$.

consider the relay node assignment for the static case that can be solved using the Hungarian method. Similarly, we also present both the greedy incremental capacity algorithm (GICA) and the optimal algorithm. The optimal solution for CARP can be obtained through the binary integer programming approach but at much higher computational complexity. The simulation results show that the GICA algorithm can produce near optimal results.

In addition, it is observed that network generally yields better coverage and throughput performance for scenarios in which all MNs start from 1 corner than from 4 corners of a disaster area. The tradeoff is that it would require longer time to clear the entire disaster area. As a conclusion, we advocate using the greedy algorithms to determine the dynamic relay placement in the deployment of disaster area wireless networks, in which real-time computation is practically more important.

Appendices

A. Proof of Theorem 2

NP-completeness applies directly not to optimization problems, however, but to decision problems, in which the answer

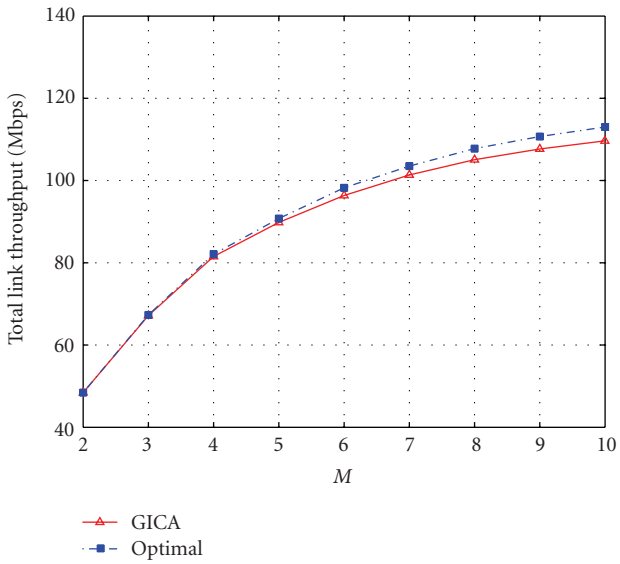

(a) At initial stage, 40 MNs are in $s_{1,1}$ at time 0, and CI values of all squares are 5

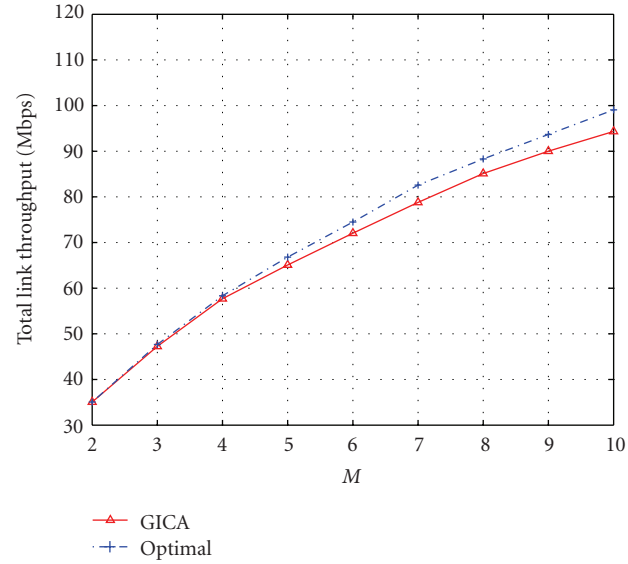

(b) At initial stage, 40 MNs are evenly deployed in $s_{1,1}, s_{1,10}, s_{10,1}, s_{10,10}$ at time 0, and CI values of all squares are 5

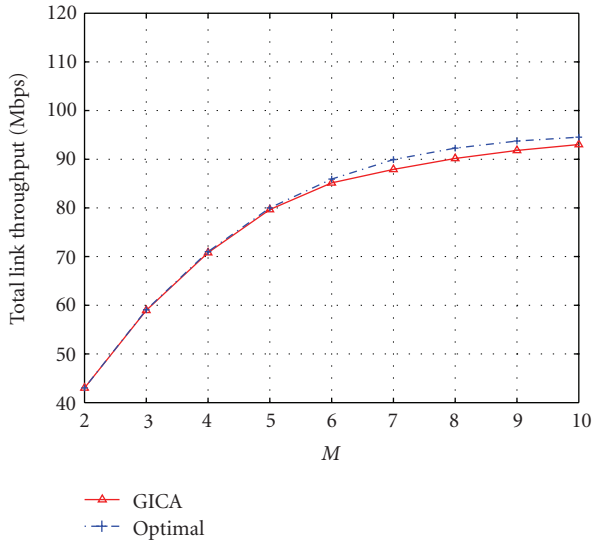

(c) At initial stage, 40 MNs are in $s_{1,1}$ at time 0, and CI values of all squares are randomly chosen between 1 and 10

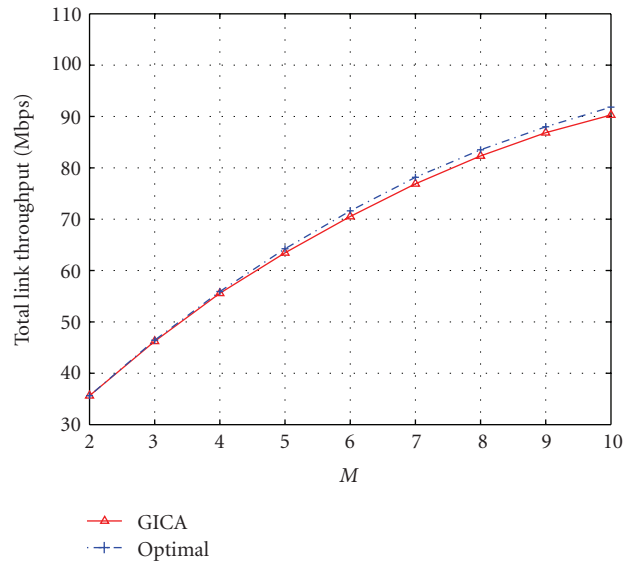

(d) At initial stage, 40 MNs are evenly deployed in $s_{1,1}, s_{1,10}, s_{10,1}, s_{10,10}$ at time 0. CI values of all squares are randomly chosen between 1 and 10

FIGURE 10: Average total link throughput over the entire relief process versus different number of RNs in four scenarios. $r = 1.5L$, $C = 10$.

is simply "yes" or "no" [24]. We first present the decision problem CORP-D associated with the CORP problem as follows. Given a set of busy squares, the number of MNs in each square, the transmission range r and M RNs each with capability C, is it possible to cover all MNs using exactly M RNs? To prove the NP-completeness of the CORP problem, it suffices to prove that the decision problem CORP-D is NP-complete.

We start by arguing that CORP-D$\in$NP. Then we prove that the CORP-D problem is NP-hard by showing that MSC$\leq_p$CORP-D, ($\leq_p$ denotes a transformation of polynomial time. MSC denotes the NP-complete minimum set cover problem). Because the CORP-D problem is both NP and NP-hard, it is NP-complete.

To show CORP-D$\in$NP, we deploy M RNs in the shared regions. Then to find if such deployment of M RNs can cover all MNs is tantamount to solving the RA-CORP problem. As the RA-CORP problem has been proved to be solved in polynomial time, CORP-D $\in$NP.

We next prove that MSC$\leq_p$CORP-D, which shows that CORP-D is NP-hard. Let $< U, Y, Z >$ be an instance of the *MSC* problem, where X denotes the collection of subsets of

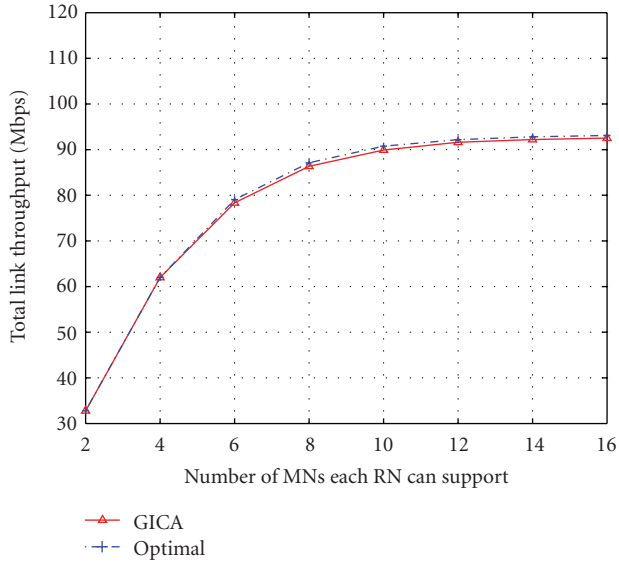

(a) At initial stage, 40 MNs are in $s_{1,1}$ at time 0, and CI values of all squares are 5

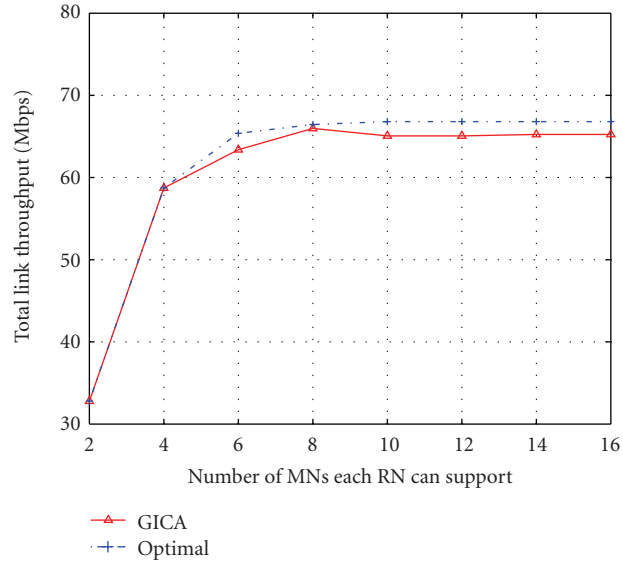

(b) At initial stage, 40 MNs are evenly deployed in $s_{1,1}, s_{1,10}, s_{10,1}, s_{10,10}$ at time 0, and CI values of all squares are 5

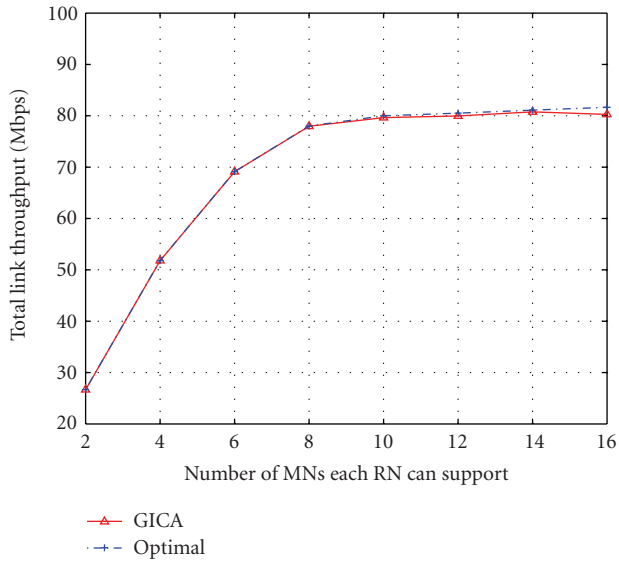

(c) At initial stage, 40 MNs are in $s_{1,1}$ at time 0, and CI values of all squares are randomly chosen between 1 and 10

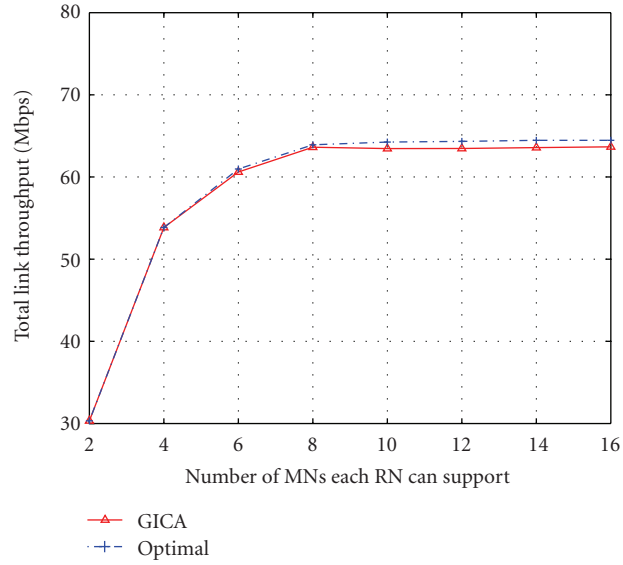

(d) At initial stage, 40 MNs are evenly deployed in $s_{1,1}, s_{1,10}, s_{10,1}, s_{10,10}$ at time 0. CI values of all squares are randomly chosen between 1 and 10

FIGURE 11: Average covering percentage over the entire relief process versus different capabilities of RNs in four scenarios. $r = 1.5L$, $M = 5$.

a set Y, Z denotes the minimum cardinality of the set U' such that $U' \subset U$ and $\cup_{u \in U'} u = Y$. To obtain an instance of the CORP-D problem we only need to define the capacity bound C for each RN. Let C be the number of all MNs. Then we build the relationship between instances of the CORP-D problem and the MSC problem as follows. (1) Each element in the set Y corresponds to one MN; (2) each shared region corresponds with one subset $u_i \in U$. (3) n_i is covered by the jth shared region if $y_i \in u_j$. Then we must prove that M RNs can cover all MNs if, and only if, there exists $U' \subset U$, such that $\cup_{u \in U'} u = Y$ and $|U'| \leq Z$.

First, suppose that N MNs in a set of busy squares can be covered by Z RNs, each with a capacity of N. Then for r_j deployed at one shared region, the corresponding subset is chosen as one element in U'. Since Z RNs can cover all N MNs, it is easy to see that $\cup_{u \in U'} u = Y$ and $|U'| \leq Z$.

Now assume that there exists $U' \subset U$, such that $\cup_{u \in U'} u = Y$ and $|U'| \leq Z$. For $u_i \in U$, we can place one RN r_i at the ith shared region. In the meantime, r_i covers n_j if $y_j \in u_i$. Since $\cup_{u \in U'} u = Y$, all N MNs are covered by the RNs. Since $|U'| \leq Z$, the number of RNs placed is no larger than Z.

Thus we have shown that the CORP-D problem is NP-complete, which completes the proof.

B. Proof of Theorem 4

We start by arguing that CARP-D∈NP (CARP-D is the decision problem associated with the CARP problem). Then we prove that CARP-D is NP-hard by showing that CORP-D$\leq_p$CARP-D. Because the problem CARP-D is both NP and NP-hard, the problem CARP is NP-complete.

To show CARP-D∈NP, we deploy M RNs in the shared regions. Then to find if such deployment of M RNs can produce the objective amount of throughput is tantamount to solving the RA-CARP problem. As the RA-CARP problem has been proved to be solved in polynomial time, the problem CARP-D∈ NP.

We next prove that CORP-D$\leq_p$CARP-D, which shows that the problem CARP-D is NP-hard. Let $\langle \mathcal{SR}, \mathcal{MN}, M, C\rangle$ and a positive integer $I \leq N$ be an instance of the CORP-D problem. To obtain an instance of the CARP-D problem we only need define the capacity of each link between one MN and RN. Let the capacity for every link between each RN and MN be 1 unit. Then we recognize the instance of the CARP-D problem the same as the instance of the CORP-D problem. This transformation surely consumes polynomial time. Subsequently, we must prove that I units of throughput can be produced if and only if I MNs can be covered by the same set of RNs.

First, suppose that I MNs in a set of busy squares can be covered by M RNs. Then for n_j covered by r_i, one link is established between n_j and r_i to produce one unit of capacity. Since I MNs are covered, it is easy to see that I units of throughput can be produced.

Now we assume that the overall network capacity is I units. Then for each link between n_j and r_i, we render r_i cover n_j. As there are I links available, each associated with one MN, I MNs can be covered by the same set of RNs.

Thus we have shown that the problem CARP-D is NP-complete, which completes the proof.

Acknowledgments

This work has been supported in part by the National Science Foundation (NSF) through Award ECS-0725522 and by the Faculty Advancement in Research Awards from WPI. This work was presented in part at 3rd Intl. Conf. Wireless Algorithms, Systems and Applications, 2008.

References

[1] W. Guo, X. Huang, and Y. Liu, "Dynamic relay deployment for disaster area wireless networks," *Wireless Communications and Mobile Computing*, 2008.

[2] H. W. Kuhn, "The hungarian method for the assignment problem," *Naval Research Logistics Quarterly*, vol. 2, no. 1-2, 1955.

[3] U. Hiroaki, T. Jun, S. Kazuki, U. Takaaki, and H. Teruo, "A manet based system for gathering location and personal information from victims in disasters," *IEIC Technical Report*, vol. 105, no. 260, pp. 13–18, 2005.

[4] K. Kanchanasut, A. Tunpan, M. A. Awal, D. K. Das, T. Wongsaardsakul, and Y. Tsuchimoto, "A multimedia communication system for collaborative emergency response operation in disaster-affected areas," Tech. Rep. 2007-1, Internet Education and Research Laboratory, Asian Insitute of Technology, Bangkok, Thailand, January 2007.

[5] D. Malan, T. Fulford-Jones, M. Welsh, and S. Moulton, "An ad hoc sensor network infrastructure for emergency medical care," in *Proceedings of the Workshop on Applications of Mobile Embedded Systems in Conjunction with the 2nd International Conference on Mobile Systems, Applications and Services (Mobisys '04)*, Boston, Mass, USA, June 2004.

[6] G. Zussman and A. Segall, "Energy efficient routing in ad hoc disaster recovery networks," *Ad Hoc Networks*, vol. 1, no. 4, pp. 405–421, 2003.

[7] Y. Shibata, Y. Sato, N. Ogasawara, and G. Chiba, "Ballooned wireless mesh network for emergency information system," in *Proceedings of the 22nd International Conference on Advanced Information Networking and Applications-Workshops (WAINA '08)*, pp. 1118–1122, Quebec, Canada, March 2008.

[8] V. Frost and B. Melamed, "Traffic modeling for telecommunications networks," *IEEE Communications Magazine*, vol. 32, no. 3, pp. 70–81, 1994.

[9] K. K. Leung, W. A. Massey, and W. Whitt, "Traffic models for wireless communication networks," *IEEE Journal on Selected Areas in Communications*, vol. 12, no. 8, pp. 1353–1364, 1994.

[10] C. Lo, R. Wolff, and R. Bernhardt, "An estimate of network database transaction volume to support universal personal communications service," in *Proceedings of the 1st International Conference on Universal Personal Communications (ICUPC '92)*, pp. 1–6, Dallas, Tex, USA, September-October 1992.

[11] R. J. Bouchard and C. E. Pyers, "Use of gravity model for describing urban travel," *Highway Research Record*, vol. 88, pp. 1–43, 1965.

[12] D. Lam, D. C. Cox, and J. Widom, "Teletraffic modeling for personal communications services," *IEEE Communications Magazine*, vol. 35, no. 2, pp. 79–87, 1997.

[13] J. G. Markoulidakis, G. L. Lyberopoulos, D. F. Tsirkas, and E. D. Sykas, "Mobility modeling in third-generation mobile telecommunications systems," *IEEE Personal Communications*, vol. 4, no. 4, pp. 41–56, 1997.

[14] P. B. Slater, "International migration and air travel: global smoothing and estimation," *Applied Mathematics and Computation*, vol. 53, no. 2-3, pp. 225–234, 1993.

[15] N. Aschenbruck, E. Gerhards-Padilla, M. Gerharz, M. Frank, and P. Martini, "Modelling mobility in disaster area scenarios," in *Proceedings of the 10th ACM Symposium on Modeling, Analysis, and Simulation of Wireless and Mobile Systems (MSWiM '07)*, pp. 4–12, Chania, Greece, October 2007.

[16] S. Nelson, A. Harris, and R. Kravets, "Eventdriven, rolebased mobility in disaster recovery networks," in *Proceedings of the 2nd Workshop on Challenged Networks (CHANTS '07)*, Montréal, Canada, September 2007.

[17] S. Kim, J.-G. Ko, J. Yoon, and H. Lee, "Multiple-objective metric for placing multiple base stations in wireless sensor networks," in *Proceedings of the 2nd International Symposium on Wireless Pervasive Computing (ISWPC '07)*, pp. 627–631, Feburary 2007.

[18] Y. Shi and Y. T. Hou, "Approximation algorithm for base station placement in wireless sensor networks," in *Proceedings of the 4th Annual IEEE Communications Society Conference on Sensor, Mesh and Ad Hoc Communications and Networks (SECON '07)*, pp. 512–519, San Diego, Calif, USA, June 2007.

[19] Y. T. Hou and Y. Shi, "Optimal base station selection for anycast routing in wireless sensor networks," *IEEE Transactions on Vehicular Technology*, vol. 55, no. 3, pp. 813–821, 2006.

[20] J. Pan, Y. T. Hou, L. Cai, Y. Shi, and S. Shen, "Topology control for wireless sensor networks," in *Proceedings of the 3rd International Workshop on Discrete Algorithms and Methods for Mobile Computing and Communications (ICDCS '99)*, Seattle, Wash, USA, August 1999.

[21] A. Pothen and C. Fan, "Computing the block triangular form of a sparse matrix," *ACM Transactions on Mathematical Software*, vol. 16, no. 4, pp. 303–324, 1990.

[22] L. A. Wolsey, *Integer Programming*, John Wiley & Sons, New York, NY, USA, 1998.

[23] A. D. Belegundu and T. R. Chandrupatla, *Optimization Concepts and Applications in Engineering*, Prentice-Hall, Upper Saddle River, NJ, USA, 1999.

[24] T. Cormen, C. Leiserson, R. Rivest, and C. Stein, *Introduction to Algorithms*, MIT Press, Cambridge, MA, USA, 2002.